

C81

### Stimulation of calcium channel function by $\alpha_2\delta$ -2 requires its metal ion-dependent adhesion (MIDAS) site

F. Hebllich, C. Canti, J. Wratten, I. Foucault, M. Nieto-Rostro, A. Davies, L. Douglas and A.C. Dolphin

Pharmacology, UCL, London, UK

In this study we have investigated properties of the membrane-anchored, but predominantly extracellular  $\alpha_2\delta$ -2 subunit of voltage-gated  $\text{Ca}^{2+}$  channels. The  $\alpha_2\delta$ -1 and  $\alpha_2\delta$ -2 subunits enhance current amplitude, increase the rate of inactivation and hyperpolarize the steady-state inactivation of high voltage-activated (HVA) currents, although their mechanism of action is not well understood. All  $\alpha_2\delta$ -2 subunits contain a Von Willebrand factor-A (VWF) domain within the extracellular  $\alpha_2$  moiety. VWF domains are present in integrins and other proteins, and contain a sequence motif representing a metal ion-dependent adhesion site (MIDAS) which confers divalent metal (usually  $\text{Mg}^{2+}$ )-dependent binding to the ligand.

tsA-201 and NG108-15 cells were transiently transfected using FuGENE. Green fluorescent protein was included to identify transfected cells. Where appropriate, solutions were designed to inhibit unwanted conductances. Data are displayed as % of control, mean  $\pm$  S.E.M.

We examined the role of the VWF domain in  $\alpha_2\delta$ -2 and in particular the importance of the MIDAS site in its functional effects. Whole-cell patch-clamp recordings from  $\text{Ca}_v1.2$  and  $\text{Ca}_v2.2$  channels, expressed in tsA-201 cells ( $H_p = -90$  mV, 10 mM  $\text{BaCl}_2$ ), demonstrate that deletion of the VWF domain and more specifically mutation of the three key amino acids responsible for divalent metal binding in the VWF domain ( $\alpha_2\delta$ -2  $\mu\text{MIDAS}$ ), completely prevented the  $\alpha_2\delta$ -2-induced enhancement of these calcium channel currents. For example, peak  $\text{Ca}_v2.2$  currents expressed with wild type  $\alpha_2\delta$ -2 were  $520 \pm 169$  % of the control in the absence of  $\alpha_2\delta$ -2 ( $n = 10$ ) whereas  $\text{Ca}_v2.2$  currents expressed with  $\alpha_2\delta$ -2  $\mu\text{MIDAS}$  were  $111 \pm 29$  % of control ( $n = 11$ ). Similar results were obtained using  $\text{Na}^+$  as charge carrier through  $\text{Ca}_v2.2$  channels (in the absence of any extracellular divalent cations). Therefore, any involvement of the MIDAS site binding of  $\text{Ca}^{2+}$  or  $\text{Mg}^{2+}$ , in the function of  $\alpha_2\delta$ -2, in relation to  $\text{Ca}_v\alpha1$  subunit expression or function, is likely to be during channel assembly or trafficking to the membrane, rather than once the channel has reached the cell surface. Furthermore, although the wild type  $\alpha_2\delta$ -2 enhanced endogenous HVA calcium currents in differentiated NG108-15 cells ( $\text{BaCl}_2$  20 mM,  $H_p = -40$  mV) to  $222 \pm 34$  % of control ( $n = 9$ ), the  $\alpha_2\delta$ -2  $\mu\text{MIDAS}$  construct had no significant effect, the current being  $86.5 \pm 14$  % of control ( $n = 10$ ).

Both immunocytochemical and cell surface biotinylation experiments show that these mutations in  $\alpha_2\delta$ -2 do not prevent their expression at the cell surface. Our future experiments will aim to determine how the mutations in the MIDAS site affect calcium channel function.

This work was supported by the MRC.

Where applicable, the experiments described here conform with Physiological Society ethical requirements.

C82

### Crucial Role of Beta Subunits for Expression and G Protein Modulation of N-Type Calcium Channels Revealed by Mutational Analysis of the I-II Loop of $\text{Ca}_v2.2$

J. Leroy, M. Richards, A.J. Butcher, M. Nieto-Rostro, W.S. Pratt, T. Davies and A.C. DOLPHIN

Pharmacology, University College London, LONDON, LONDON, UK

High-voltage activated calcium channels (HVA) are heteromultimers composed of a main pore-forming  $\text{Ca}_v\alpha1$  subunit associated with auxiliary subunits  $\beta$  and  $\alpha_2\delta$ . The  $\beta$  subunits modulate biophysical properties of the channels and promote the voltage-dependence of modulation of N-type calcium channels by G proteins (Meir et al., 2000). They bind to an interaction site of nine amino-acids (QQXExxLxGYxxWlxxxE), the Alpha-Interaction Domain (AID), conserved in the I-II loop of the  $\text{Ca}_v\alpha1$  subunit of all HVA calcium channels. By mutating W391 to A in the AID of  $\text{Ca}_v2.2$ , we confirmed that this amino-acid is essential for  $\beta1b$  subunit binding (Fig. 1), for plasma membrane expression and for modulation of the biophysical properties of  $\text{Ca}_v2.2$  channels.

Whereas robust currents were recorded co-expressing  $\text{Ca}_v2.2$  with  $\beta1b$  ( $-219.47 \pm 41$  pA/pF at +20 mV; (mean  $\pm$  S.E.M,  $n=12$ ), co-transfection of  $\text{Ca}_v2.2$ (W391A) with  $\beta1b$  induced small currents ( $-31.75 \pm 7.4$  pA/pF at +20 mV;  $n=11$ ). Moreover, without  $\beta$ ,  $\text{Ca}_v2.2$  produced small but recordable currents ( $-8.22 \pm 1.1$  pA/pF at +20 mV;  $n=13$ ) while the currents were negligible when  $\text{Ca}_v2.2$ (W391A) was expressed alone ( $n=21$ ), suggesting that some endogenous  $\beta$  may be present in tsA-201 cells and trafficking wild type  $\text{Ca}_v2.2$ . Activating with 100 nM quinpirole a Dopamine D2 receptor co-transfected in tsA-201 cells with  $\text{Ca}_v2.2$ ,  $\beta1b$  and  $\alpha_2\delta2$  allowed us to study the G protein modulation of N-type calcium channels. For the wild type channel, quinpirole induced an inhibition of  $53.5 \pm 3.8$  % ( $n=12$ ) of the recorded currents and a +7 mV shift of its activation. Time constant of activation ( $\tau$ ) was slowed from  $2.45 \pm 0.55$  ms to  $4.64 \pm 0.48$  ms and prepulse potentiation was observed. The  $\text{Ca}_v2.2$ (W391A) mutant was still inhibited ( $46.4 \pm 8$  %  $n=11$ ) by G-proteins and a positive shift of +6.5 mV for its activation still occurred but the slowed activation kinetics and prepulse potentiation were not observed for this mutant. However, in contrast to expectation from the crystal structure, mutation of another amino-acid within the AID, Y388 to S did not affect channel properties or its G-protein modulation. These results confirm that the W391 is crucial for  $\beta$  subunits binding to the I-II linker of  $\text{Ca}_v2.2$ , and show that no  $\text{Ca}_v2.2$  is functional at the plasma membrane in the complete absence of interaction with a  $\beta$  subunit. The results also provide evidence for the role of  $\beta$  subunits in the voltage-dependence of modulation of N-type calcium channels by G protein-coupled receptors.

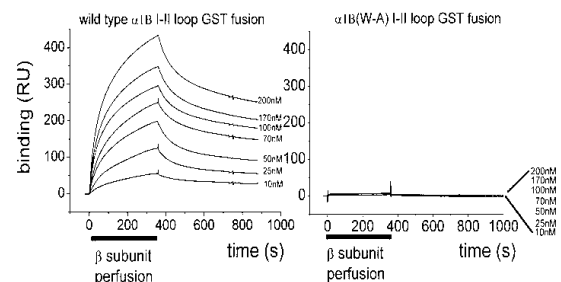


Figure 1: Examples of Biacore 2000 sensorgrams for comparison of purified Beta1b binding to a GST- $\text{Ca}_v2.2$  I-II loop (left)  $\text{Ca}_v2.2$ (W391A) I-II loop (right).

Meir et al. (2000). *Biophys. J.* 79, 731-746.

Supported by the Wellcome Trust.

Where applicable, the experiments described here conform with Physiological Society ethical requirements.

C83

### Protein kinase C mediates up-regulation of Na<sub>v</sub>1.9 (NaN) in sensory neurones

M.D. Baker

Molecular Nociception Group, University College London, London, UK

The persistent tetrodotoxin-resistant (TTX-r) Na<sup>+</sup> current, attributed to Na<sub>v</sub>1.9 (NaN), is expressed in peripheral nociceptive neurones (e.g. Fjell *et al.* 2000) and at unmyelinated nerve endings (Black & Waxman, 2002). It activates at membrane potentials near rest and can be dramatically up-regulated by at least one G-protein pathway, leading to depolarization, a more negative voltage-threshold for action potential induction and spontaneous activity in small diameter DRG neurones in culture (Baker *et al.* 2003). In order to clarify the mechanism of this functional up-regulation, experiments were performed on small (<25 µm apparent diameter) DRG neurones from P21 rat and adult WT and Na<sub>v</sub>1.8 null mouse, maintained in culture for 1 to 2 days. All voltage-clamp recordings were made in the presence of 250 nM external TTX. With 3 mM ATP internal, intracellular GTP-γ-S (500 µM) induced a near 300 % average increase in Na<sub>v</sub>1.9 (NaN) current amplitude in Na<sub>v</sub>1.8 null neurones over 5 minutes, an effect abolished by including the inhibitor PKC 19-36 in the internal solution (0.5 - 5 µM), *n* = 10 and 6, respectively; *p* = 0.035, 2-way repeated measures ANOVA. Incorporation of 1-oleoyl-2-acetyl-sn-glycerol (OAG) (25 µM) in an intracellular solution also containing GDP (500 µM) and ATP (3 mM), caused an increase in Na<sup>+</sup> current recorded in WT neurones at -40 mV and more negative (Fig. 1), that did not occur in neurones with GDP and ATP only (*n* = 9 and 9, respectively; *p* < 0.03, Fisher exact test). In perforated-patch, voltage-clamp recordings from WT neurones, superfusion of dB-cAMP (1 mM) had no effect on the current, whereas exposure to phorbol 12-myristate 13-acetate (PMA; 1 µM) induced up-regulation in the same neurones (*n* = 2) consistent with the involvement of PKC but not PKA. Conversely, the major TTX-r Na<sup>+</sup> current, Na<sub>v</sub>1.8, was unaffected by exposure to PMA (*n* = 3). Finally, superfusion of ATP up-regulated Na<sub>v</sub>1.9 (NaN) (*n* = 6), with an apparent *K*<sub>d</sub> of 18.2 ± 4.6 µM (mean ± s.e.m., *n* = 3), possibly consistent with a P2Y receptor, Gq/11 coupled pathway. Sustained increases in nociceptor excitability caused by ATP might therefore be explained by the up-regulation of Na<sub>v</sub>1.9

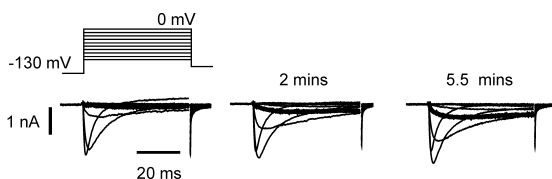


**Figure 1.** OAG (25 µM) internal induces up-regulation of TTX-r Na<sup>+</sup> current at negative membrane potentials during a conventional whole-cell, voltage-clamp experiment in a WT neurone. Current evoked at -40 mV (more negative than the activation threshold for Na<sub>v</sub>1.8) is indicated by a thicker trace.

Fjell J *et al.* (2000) *Neuroreport* 11, 199-202.

Black JA & Waxman SG (2002) *Exp. Eye Res.* 75, 193-199.

Baker MD *et al.* (2003) *J. Physiol.* 548, 373-382.

I acknowledge the support of the Wellcome Trust and thank John Wood for the Na<sub>v</sub>1.8 nulls.

Where applicable, the experiments described here conform with Physiological Society ethical requirements.

C84

### Localisation of neuronal sodium channels in rat ventricular cardiomyocytes

L.Q. Yang<sup>1</sup>, J. Gorelik<sup>2</sup>, S.E. Harding<sup>1</sup>, Y.E. Korchnev<sup>2</sup> and H.P. Ducholier<sup>3</sup>

<sup>1</sup>NHLI Division, Imperial College, LONDON, UK, <sup>2</sup>MRC - Clinical Sciences Centre, Imperial College, LONDON, UK and <sup>3</sup>Institut de Physiologie et Biologie Cellulaire, UMR 6187 CNRS - Université de Poitiers, POITIERS, France

In the heart, excitation-contraction coupling begins with the activation of sodium channels underlying the rapid rise of action potential and its propagation. Classical cardiac sodium channels are tetrodotoxin (TTX)-insensitive but recent cytoimmunohistochemical labelling (Maier *et al.*, 2002) suggest the presence of neuronal-type sodium channels in the t-tubules whereas TTX-resistant channels are preferentially localised at intercalated disks. However, the interpretation of immunohistochemical data as regards the precise localisation of sparse membrane proteins is not straightforward. We thus set out to obtain more direct functional evidence using 'Scanning Ion Conductance Microscopy' (SICM) combined with 'smart patch-clamp' as applied for calcium channels in heart cells (Shevchuk *et al.*, 2001). SICM images were recorded from both control and detubulated ventricular cardiomyocytes (Brette *et al.* 2002) isolated from Spague-Dawley rats. This permitted patch t-tubules openings in addition to the classical patching at random on the cell surface. With grayanotoxin (100 µM) in the pipette allowing steady-state activation, single-channel events of 11 pS were observed with a higher rate of success when patching t-tubules openings. We then compared the TTX-sensitivity of whole-cell sodium currents of control and detubulated cells. Bath application of 200 nM TTX reduced the sodium current peak of control cells (Fig. 1A) by 18±5 % (SEM, *n* = 12) whereas the effect was insignificant in detubulated cells. This was matched by a parallel decrease of membrane capacitance of ~30% for the detubulated cells. The peak of the remaining current of control cells (after TTX addition) occurred slightly earlier than the total sodium current and fast inactivation decay was accelerated (1.3 vs. 3 ms, Fig. 1B), as expected for neuronal, TTX-sensitive sodium channels. This study provides independent functional evidence for neuronal-type sodium channels in heart cells where they play the likely role of rapidly and synchronously couple t-tubules and cell surface depolarisations.

Maier SB *et al.* (2002) *Proc. Natl. Acad. Sci. USA* 99, 4073-4078.

Shevchuk AI *et al.* (2001) *Biophys. J.* 81, 1759-1764

Brette F *et al.* (2002) *J. Physiol. Heart Circ. Physiol.* 283, H1720-H1728.

We thank MJ Lab, D Sanchez, AI Schevchuk and I Vodyanoy for advices and help. Supported by the ISIS fellowship scheme of the BBSRC and the British Heart Foundation.

Where applicable, the experiments described here conform with Physiological Society ethical requirements.

---

C85

### Revealing the linkage (contribution) of each kinetic state in the gating mechanisms for ion channels to the exponential components in the observed dwell-time distributions

C. Shelley and K. Magleby

Department of Physiology and Biophysics, University of Miami School of Medicine, Miami, FL, USA

Ion channels play key roles in a many physiological processes such as the integration of information in neurones, propagation of action potentials, synaptic transmission. The gating of ion channels can be described by reaction mechanisms with discrete kinetic states. Whereas it is the properties of the kinetic states that are needed to describe gating, the information obtained from the analysis of single channel currents gives open and closed dwell-time distributions, which are described by sums of exponential components. In theory, the number of components will equal the number of open and closed kinetic states (i.e. a model with four kinetic open states will produce an open interval dwell time distribution described by the sum of four exponential components). However, not all of the kinetic states may be detected. Furthermore, the relationship between the dwell-time distributions and the kinetic states is complex because all of the rate constants in the model can contribute to each component in the dwell-time distributions (Colquhoun & Hawkes, 1982). The purpose of this study is to relate kinetic states to exponential components.

Using simulations of Markov gating mechanisms, we investigate the relationships between the exponential components and the kinetic states. The linkage between components and states is defined in terms of the proportion of time a given kinetic state contributes to each exponential component, and thus ranges from 0, (no linkage) to 1, (complete linkage), and also as the mean number of sojourns to each kinetic state for each interval in a given exponential component.

For the model in Fig. 1, the calculated time linkages between the lifetime of closed state 1 and the fast and slow time constants was 0.91 and 0.66, respectively. The time linkage between closed state 2 and the fast and slow closed components was 0.093 and 0.34, respectively. The inclusion of missed events (0.2 ms dead time) reduced the linkage of closed state 1 to ~0.6 for both the fast and slow components, but had little effect on the linkage between closed state 3 and the two components.

Under certain conditions, the time constants of the specified components obtained from dwell time distributions can be approximated by the lifetimes of certain states, and for other conditions there is much less linkage. For model 1 it was found that to obtain a time linkage of 0.95 between the lifetime of shut state 2 and the slowest shut time component, the lifetime of shut state 2 had to be at least 33-fold greater than the lifetime of shut state 2.

In addition, it is shown graphically why the time constant of a component can be considerably faster than the mean lifetime of any of the states in the model. An understanding of the relationships between components and states will aid in the interpretation of single channel dwell-time distributions.

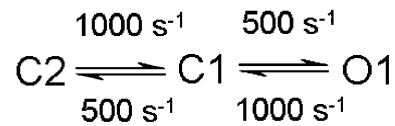


Figure 1. Model used to examine linkages between state lifetimes and the time constants of the exponential components.

Colquhoun, D. & Hawkes, A.G. (1982). Proc. Trn. R Soc Lond B 300, 1-59.

This work was supported by a Lois Pope LIFE fellowship to CS and NIH grant AR32805 to KLM.

Where applicable, the experiments described here conform with Physiological Society ethical requirements.

---

C86

### Dominant negative effects of $\beta 3$ subunit incorporation on recombinant neuronal nicotinic receptors and on nicotinic responses of rat hippocampal neurones in culture

S. Broadbent, M. Beato, P.J. Groot-Kormelink and L.G. Sivilotti

Dept of Pharmacology, UCL, London, UK

The  $\beta 3$  neuronal nicotinic subunit is expressed in discrete regions of the brain, such as the *substantia nigra*, but the functional consequences of its incorporation into nicotinic receptors (nAChRs) remain unclear. We have previously shown that recombinant receptors expressed from  $\alpha 3$ ,  $\beta 4$  and  $\beta 3$  subunits contain a single copy of  $\beta 3$  and have properties very similar to those of the background  $\alpha 3\beta 4$  combination (Boorman *et al.*, 2000; 2003). Here we examine the effects of co-expressing  $\beta 3$  together with other nAChR subunit combinations, particularly those that are likely to be expressed in the central nervous system.

Recombinant nAChRs were expressed in *Xenopus* oocytes by injection of excess cRNA for  $\beta 3$  together with cRNA for  $\alpha 2\beta 2$ ,  $\alpha 2\beta 4$ ,  $\alpha 3\beta 2$ ,  $\alpha 3\beta 4$ ,  $\alpha 4\beta 2$ ,  $\alpha 4\beta 4$  or  $\alpha 7$ . Currents evoked by ACh, bath-applied at a saturating concentration of 1 mM, were recorded by two-electrode voltage-clamp.

Adding  $\beta 3$  produced an almost complete suppression of ACh responses for all combinations, except  $\alpha 3\beta 4\beta 3$ . Depending on the combination, the maximum response to ACh was reduced by between  $88 \pm 4$  to  $100 \pm 0$  % ( $n = 5-24$ ). We investigated the cause of this effect by using a mutated  $\beta 3$  subunit carrying a 'gain-of-function' valine to serine mutation in residue 9' of the pore-lining region. When this mutant  $\beta 3^{V9S}$  subunit was expressed, maximum ACh responses were comparable to those obtained in the absence of  $\beta 3$ . The properties of dose-response curves from  $\beta 3^{V9S}$ -containing receptors were consistent with the insertion of a single copy of  $\beta 3$ .

We next tested whether  $\beta 3$  had the same effect in rat neurones by transfecting primary hippocampal cultures (from E18 embryos, donors killed humanely following Schedule 1) with

cDNA for either  $\beta 3$  (wild type or V9'S) or  $\alpha 7$ , together with EGFP (as a transfection marker). Under whole-cell clamp, untransfected cells (20 out of 22) showed typical  $\alpha 7$ -like responses to U-tube applications of 1-3 mM ACh. The amplitude of these responses was increased approximately ten-fold by transfection of  $\alpha 7$  (26 out of 26 green cells). In neurones transfected with wild type  $\beta 3$ , responses to ACh were completely suppressed (28 out of 32 cells), whereas in 47 out of 52 cells transfected with  $\beta 3^{V9'S}$ , an  $\alpha 7$ -like response to ACh was detectable.

In conclusion, dominant negative effects of wild-type  $\beta 3$  are observed in all classes of oocyte-expressed nAChRs (except  $\alpha 3\beta 4$ ) and in rat hippocampal neurones. This effect is likely to be due to a lower open probability of receptors that incorporate this subunit.

Boorman *et al.* (2000) *J. Physiol.* 529, 567-78

Boorman *et al.* (2003) *J. Biol. Chem.* 278, 44033-40

This work was supported by the Wellcome Trust (grant 064652) and the MRC (SB and MB)

Where applicable, the experiments described here conform with Physiological Society ethical requirements.

tude or kinetics of the M-current was not altered when cells were pre-incubated in PMT (500 ng ml<sup>-1</sup>) for 18-24 hours. Concentration inhibition curves to the muscarinic agonist oxotremorine-M were generated in control, PMT and PMT(C1165S) mutant pretreated cells. IC<sub>50</sub>s were (geometric mean and 95% confidence limits) 1.32 (0.65-2.67)  $\mu$ M, 0.07 (0.02-0.22)  $\mu$ M and 0.30 (0.14-0.67)  $\mu$ M respectively. The slopes were (mean  $\pm$  sem) 0.75  $\pm$  0.16 (n=6) for control, 0.90  $\pm$  0.15 (n=9) for PMT and 0.84  $\pm$  0.15 (n=6) for PMT (C1165S) pre-treated cells. Voltage dependent norepinephrine inhibition of N-type (Cav2.2) calcium channel current was not altered by pre-treatment with PMT. These data support the idea that one of the actions of PMT is to enhance the action of Gq, in part by phosphorylation.

Baldwin *et al.* (2003) *J. Biol. Chem.* 278, 32719-32725.

Haley *et al.* (1998) *J. Neurosci.* 18, 4521-4531.

Orth *et al.* (2004) *J. Biol. Chem.* 279, 34150-34155.

Supported by the MRC. We thank Prof. Lax (KCL) for the PMT(C1165S) mutant.

Where applicable, the experiments described here conform with Physiological Society ethical requirements.

## C87

### ***Pasteurella multocida* toxin modulates M1 muscarinic receptor mediated M current (Kv7) inhibition in rat sympathetic neurones**

J. Robbins<sup>1</sup>, J. Reilly<sup>2</sup> and D.A. Brown<sup>2</sup>

<sup>1</sup>Wolfson Centre for Age Related Diseases, King's College, London, UK and <sup>2</sup>Pharmacology, University College, London, UK

*Pasteurella multocida* toxin (PMT) is a bacterial toxin that mediates at least some of its effects via actions on the G-protein, Gq (Baldwin *et al.*, 2003) and shows selectivity for Gq over G11 (Orth *et al.*, 2004). Inhibition of M-current by M1 muscarinic receptor activation in rat superior cervical ganglion (SCG) neurones has been shown to be primarily mediated by Gq, rather than G11 (Haley *et al.*, 1998). In this study we have investigated the acute and chronic effects of PMT and a non toxic mutant PMT(C1165S) on muscarinic receptor-induced M-current inhibition.

SCGs (isolated from rats killed by approved Schedule 1 methods) were cultured for 2-4 days on laminin coated plastic dishes (for electrophysiology) or glass coverslips (for immunocytochemistry). Control and PMT (Calbiochem) treated cells were exposed to rabbit anti rat Gq and G11 antibodies overnight at 4°C followed by a donkey anti rabbit FITC secondary antibody for 1 hour. Amphotericin-perforated patch recording were performed on cells superfused at 23°C with a solution containing (mM): NaCl 144, KCl 2.5, MgCl<sub>2</sub> 0.5, CaCl<sub>2</sub> 2, Hepes 5, glucose 10, TTX 0.0005, pH 7.4. Patch pipettes were filled with a solution containing (mM): K acetate 80, KCl 30, Hepes 40, MgCl<sub>2</sub> 3, EGTA 3, CaCl<sub>2</sub> 1, pH 7.2. Cells were clamped at -20 mV and deactivating M-current tails evoked by 1 second hyperpolarizing steps to -50 mV every 30 seconds.

Gq antibody labelling was more intense than that for G11 in all cells tested. There was no qualitative difference in the labelling of Gq or G11 between control or PMT treated (500 ng ml<sup>-1</sup>, 24 hours at 37°C) cells.

Acute applications (1-10 min) of PMT (100 ng ml<sup>-1</sup>) had no effect on the amplitude of the M-current (n=4) and the ampli-

## C88

### **Ca<sup>2+</sup>- and volume-sensitive chloride currents are differentially regulated by agonists and store-operated Ca<sup>2+</sup> entry**

A. Zholos<sup>1</sup>, B. Beck<sup>1</sup>, V. Sydorenko<sup>1</sup>, L. Lemonnier<sup>1</sup>, P. Bordat<sup>2</sup>, N. Prevarskaya<sup>1</sup> and R. Skryma<sup>1</sup>

<sup>1</sup>Laboratoire de Physiologie Cellulaire, INSERM EMI 0228, USTL, Villeneuve d'Ascq, France and <sup>2</sup>Centre de Recherche, Pierre Fabre Dermocosmetique, Castanet-Tolosan, France

Using intracellular Ca<sup>2+</sup> imaging and patch-clamp techniques we investigated the effects of histamine, ATP, cell swelling induced by hypotonic solution (HTS; 200 mosmol/l) and thapsigargin (TG)-induced store-operated Ca<sup>2+</sup> entry (SOCE) on chloride currents in human keratinocytes (an immortalized, non-tumour HaCaT cell line). The effects of ATP and histamine were of primary interest since HaCaT cells express H<sub>2</sub> histamine and P2Y<sub>2</sub> purinergic receptors coupled to the phosphoinositide pathway and since keratinocytes are typically exposed to these substances during skin injury, inflammatory skin diseases and allergic reactions. In intact cells receptor agonists as well as TG induced a transient elevation of [Ca<sup>2+</sup>]<sub>i</sub> in a Ca<sup>2+</sup>-free medium followed by a secondary [Ca<sup>2+</sup>]<sub>i</sub> rise upon Ca<sup>2+</sup> readmission due to SOCE. Agonists activated two kinetically distinct currents which showed different voltage dependence and were identified as Ca<sup>2+</sup>-activated (I<sub>Cl(Ca)</sub>) and volume-regulated (I<sub>Cl(swell)</sub>) chloride currents. At 100  $\mu$ M 5-nitro-2-(3-phenylpropylamino) benzoic acid (NPPB) and 4,4'-diisothiocyanato-stilbene-2,2'-disulfonic acid (DIDS) more efficiently inhibited I<sub>Cl(Ca)</sub> and I<sub>Cl(swell)</sub>, respectively (90 $\pm$ 9% vs. 58 $\pm$ 3% inhibition of I<sub>Cl(Ca)</sub> and 33 $\pm$ 14% vs. 97 $\pm$ 2% inhibition of I<sub>Cl(swell)</sub> by NPPB and DIDS, respectively; n=4). The PLC inhibitor U-73122 blocked both agonist- and cell swelling-induced I<sub>Cl(swell)</sub> (at 1  $\mu$ M by 72 $\pm$ 14%; n=5 and 75 $\pm$ 4%; n=3, respectively) while its inactive analogue U-73343 had no effect. I<sub>Cl(swell)</sub> could be directly activated by OAG, a cell-permeable diacylglycerol analogue, but not by InsP<sub>3</sub> infusion; protein kinase

C also had no role in its regulation. Agonists had no effect on 100  $\mu$ M OAG-induced current while HTS-induced current was insensitive to both agonists and OAG (in all cases current amplitude changed by less than 5%). Thus, agonists, OAG and cell swelling induced  $I_{Cl,swell}$  in a non-additive manner suggesting their convergence on a common pathway. Moreover, both  $I_{Cl,swell}$  and  $I_{Cl(Ca)}$  showed no or very little overlap (i.e. simultaneous activation) although various manoeuvres could induce these currents sequentially in the same cell. TG-induced SOCE strongly potentiated  $I_{Cl(Ca)}$  but abolished  $I_{Cl,swell}$  providing a clue for this paradox. Thus, we have established for the first time using keratinocyte model that  $I_{Cl,swell}$  can be physiologically activated under isotonic conditions by receptors coupled to the phosphoinositide pathway. These results also suggest a novel function for SOCE which can operate as a "selection" switch between closely localized channels; this way cells can translate a graded  $Ca^{2+}$  entry via SOC channels into different ion channel responses.

Where applicable, the experiments described here conform with Physiological Society ethical requirements.

---

C89

### The differential effects of $\beta$ 1- and $\beta$ 2-subunits on BK channel activity are associated to their transmembrane and cytosolic domains

P. Orio, P. Rojas, I. Carvacho and R. Latorre

Centro de Estudios Científicos, Valdivia, Chile

High conductance, calcium- and voltage-activated potassium (BK) channels are widely expressed in mammals. In some tissues, the biophysical properties of BK channels are highly affected by coexpression of regulatory ( $\beta$ )-subunits.  $\beta$ 1- and  $\beta$ 2-subunits increase the calcium sensitivity and  $\beta$ 1-subunit also decreases the voltage dependence of the channel. We further characterized the effects of the  $\beta$ 1- and  $\beta$ 2-subunits on the calcium- and voltage sensitivity of the channel, analyzing the data in the context of an allosteric model for BK channel activation by calcium and voltage (Horrigan & Aldrich, 2002). For a better characterization of the effects on channel activation, a  $\beta$ 2-subunit without its N-type inactivation domain ( $\beta$ 2IR) was used.  $\alpha$ - (pore-forming) and  $\beta$ -subunits were coexpressed in *X. laevis* oocytes and currents were studied with the patch clamp technique. In the absence of calcium the limiting voltage dependence for steady-state open probability, unrelated to voltage sensor movements, is not affected by any of the studied  $\beta$ -subunits ( $\alpha$  alone: 0.3 electronic charges ( $e$ ),  $\alpha + \beta$ 1: 0.33 $e$ ,  $\alpha + \beta$ 2IR: 0.29 $e$ ). On the other hand, the maximum slope of the  $\ln(P_o)/dV$  relationship, strictly related to voltage sensor-dependent activation, is significantly reduced only by the  $\beta$ 1-subunit ( $\alpha$ : 1.94 $\pm$ 0.08 $e$ ,  $\alpha + \beta$ 1: 1.40 $\pm$ 0.3 $e$ ,  $\alpha + \beta$ 2IR: 1.84 $\pm$ 0.07 $e$ ). When the data is fitted to the allosteric model for voltage activation, the  $\beta$ 1-subunit reduces the voltage dependence of the voltage sensor activation ( $z_j$ ) ( $\alpha$ : 0.6 $e$ ,  $\alpha + \beta$ 1: 0.39 $e$ ,  $\alpha + \beta$ 2IR: 0.55 $e$ ). When the allosteric model is expanded to include the activation by calcium, the reduction of  $z_j$  accounts for most of the effects of the  $\beta$ 1-subunit on the channel steady-state activation, surprisingly including the increase of the apparent calcium sensitivity. In the case of the  $\beta$ 2IR-subunit, an increase of the allosteric coupling factors for channel activation

by calcium and voltage is required to account for its effects. The study of chimeras between  $\beta$ 1- and  $\beta$ 2IR-subunits shows that the differences between these  $\beta$ -subunits are associated to their transmembrane and/or intracellular domains. We conclude that the transmembrane and intracellular domains of the  $\beta$ 1-subunit modulate the movement of the voltage sensors of BK channel and that the  $\beta$ 2IR-subunit increases the channel's apparent calcium sensitivity by a different mechanism than the  $\beta$ 1-subunit. Horrigan FT & Aldrich RW (2002). *J Gen Physiol* 120, 267-305.

Supported by Fondecyt 103-0830 (RL). The Centro de Estudios Científicos is a Millennium Institute and is funded in part by a grant from Fundación Andes.

Where applicable, the experiments described here conform with Physiological Society ethical requirements.

---

C90

### A 4-AP-sensitive current is differentially modulate by chronic hypoxia in right and left rat coronary artery myocytes

M. Gautier and P. Bonnet

Laboratoire de Physiopathologie de la Paroi Arterielle, Université François Rabelais - UFR Médecine, Tours, France

Chronic hypoxia was demonstrated to induce right ventricular hypertrophy and changes in right coronary artery blood flow. Moreover, it induced a vasodilation in the whole heart, but it is not clear whether hypoxia-mediated vasodilation occurs (Thorne et al., 2004). We hypothesized that chronic hypoxia could modify reactivity of right coronary artery myocytes by  $K^+$ -current modulation. Seven weeks old male Wistar rats were housed in a hypoxic chamber during 3 weeks ( $PO_2 = 75$  mmHg) and were compared to normoxic rats ( $PO_2 = 150$  mmHg). Animals were killed by pentobarbital injection (60 mg.kg<sup>-1</sup> ip). The descending anterior branch of the left coronary artery and the main branch of the right coronary artery were dissected. Coronary artery myocytes were isolated by enzymatic digestion as previously described (Barbe et al., 2002). Outward currents were recorded using Patch-Clamp technique. They were generated by membrane depolarization pulse of 8 mV (400 ms) from a holding potential of -60 mV and up to +60 mV. Results are expressed as mean $\pm$ S.E.M., n represents the number of cells. Outward current-density in right coronary artery (RCA n=22) myocytes was higher than in left coronary artery (LCA n=15) myocytes (21.3 $\pm$ 2.6 pA/pF vs 14.9 $\pm$ 3.1 pA/pF). Moreover RCA myocytes were less depolarized than LCA myocytes (-24.8 $\pm$ 1.2 mV vs -20.6 $\pm$ 1.2 mV). Chronic hypoxia induced a decrease in outward current-density in RCA myocytes (13.9 $\pm$ 1.1 pA/pF n=14) and it depolarized the cell membrane (-17.7 $\pm$ 1.9 mV). In opposite, chronic hypoxia increased outward current-density in LCA myocytes (27.5 $\pm$ 4.7 pA/pF n=8) and hyperpolarized the cell membrane (-25.0 $\pm$ 1.9 pA/pF). To further characterise the hypoxic-sensitive current, we used 4-AP, a well known blocker of voltage-gated  $K^+$ -channels. The 4-AP-sensitive current was significantly lower in LCA (n=7) compared to RCA (n=12) myocytes (4.8 $\pm$ 2.3 pA/pF vs 9.6 $\pm$ 2.6 pA/pF). We found that chronic hypoxia decreased the 4-AP-sensitive current in RCA myocytes (4.5 $\pm$ 0.9 pA/pF n=8) but it increased the 4-AP-sensi-

tive current in LCA myocytes ( $11.5 \pm 5.1$  pA/pF  $n=3$ ). We conclude that chronic hypoxia has opposite effects on 4-AP-sensitive current on right and left coronary myocytes. Whilst this current was decreased in RCA myocytes it was increased in LCA myocytes. This difference is probably linked to a differential expression of Kv-channels sensitive to hypoxia in LCA and RCA myocytes. Identity of these channels remains to be discovered.

Barbe et al. (2002) *Am J Physiol Heart Circ Physiol* **282**: H2031-8

Thorne et al. (2004) *Cell Calcium* **36**: 201-8

This work is supported by l'Agence de l'Environnement et de la Maitrise de l'Energie (ADEME) and Pfizer Laboratories, Amboise, France.

*Where applicable, the experiments described here conform with Physiological Society ethical requirements.*

## C91

### **TREK-1 is resistant to hypoxia : identification of an artefact caused by gas bubbling of arachidonic acid solutions**

K.J. Buckler<sup>1</sup> and E. Honore<sup>2</sup>

<sup>1</sup>University Laboratory of Physiology, Oxford University, Oxford, UK and <sup>2</sup>Institut de Pharmacologie Moléculaire et Cellulaire, CNRS, Sophia Antipolis, France

TREK-1 is a member of the  $K_{2P}$  channel family that is mechano-, heat-, pH-, anaesthetic- and lipid-sensitive. It is highly expressed in the central nervous system and probably encodes one of the arachidonic acid activated  $K^+$ -channels. Polyunsaturated fatty acids and lysophospholipids protect the brain against ischemia. Since both are openers of TREK-1, it has been suggested that this  $K_{2P}$  channel is directly involved in neuroprotection (Patel & Honore, 2001). Recently, however this view has been challenged by a report claiming that TREK-1 and its activation by arachidonic acid is inhibited by hypoxia (Miller et al. 2003). We have reinvestigated this phenomenon.

HEK 293 cells were transiently transfected with plasmids containing DNA encoding mouse TREK-1 (pCi IRES-CD8-mTREK-1) and enhanced green fluorescent protein (pCi IRES-EGFP-mTREK-1). Whole cell voltage-clamp recordings were conducted in HEPES buffered media at room temperature 48-72 hrs post transfection. Pipette filling solutions contained 5 mM ATP.

In preliminary experiments the effects of arachidonic acid upon TREK-1 appeared to be greatly suppressed by bubbling solutions with a wide range of gas mixtures including air. Upon further investigation we found that gas bubbling resulted in the loss of  $78\% \pm 1\%$  (mean  $\pm$  SEM,  $n=4$ ) of 3H arachidonic acid from the bulk phase of solution within an hour. We suggest that this may be due to the amphipathic nature of arachidonic acid favouring its redistribution to the air water interface aided by the passage of bubbles through solution.

By using a gas equilibration method which avoided bubbling induced loss of arachidonic acid from solution, we found mTREK-1 to be strongly activated by arachidonic acid under both normoxic and hypoxic conditions. Mean mTREK-1 current measured at 0 mV in the presence of 10  $\mu$ M arachidonic acid was  $4.6 \pm 1.2$  nA in air equilibrated solutions and  $4.7 \pm 1.0$  nA in hypoxic solutions ( $N_2$  equilibrated,  $PO_2 < 4$  torr); both values were significantly ( $P < 0.02$ , paired Student's t test) greater than their respective control levels ( $0.37 \pm 0.1$  nA in air &  $0.4 \pm 0.1$  nA in  $N_2$ ,  $n=6$ ). Indeed hypoxia had no significant effect upon mTREK-1 currents under either control conditions or in the presence of arachidonic acid.

These data demonstrate that TREK-1 is strongly activated by arachidonic acid even under hypoxic conditions and thus support the proposed role for TREK-1 in ischemic neuroprotection. Miller P, Kemp PJ, Lewis A, Chapman CG, Meadows H & Peers C (2003). *J. Physiol.* **548**, 31-37.

Patel AJ & Honore E (2001) *Trends Neurosci.* **24**, 339-346.

This work was funded by the British Heart Foundation and the CNRS.

*Where applicable, the experiments described here conform with Physiological Society ethical requirements.*

## PC72

**Functional comparison of the calcium activated cation channels TRPM4 and TRPM5.**

N.D. Ullrich, K. Talavera, J. Prenen, T. Voets and B. Nilius

*Department of Physiology, Katholieke Universiteit Leuven, Leuven, Belgium*

In this study, we provide a direct comparison of the gating characteristics and blocker sensitivity of mouse TRPM4 and TRPM5, two  $\text{Ca}^{2+}$ -activated nonselective cation channels of the melastatin related TRP (transient receptor potential) family. HEK293 cells were grown under standard tissue culture conditions and transiently transfected with a bicistronic vector containing GFP and either TRPM4 or TRPM5. Data are presented as mean  $\pm$  S.E.M. Using combined whole-cell patch clamp technique and flash photolysis of caged  $\text{Ca}^{2+}$  for intracellular  $\text{Ca}^{2+}$  measurements, we investigated the dependence of current activation on the intracellular  $\text{Ca}^{2+}$  concentrations. TRPM5 currents revealed higher sensitivity to  $[\text{Ca}^{2+}]_i$  than TRPM4: TRPM5 was activated by submicromolar concentrations of  $\text{Ca}^{2+}$  with values of  $0.9 \pm 0.13 \mu\text{M}$  ( $n=5$ ) compared to the higher activation threshold of TRPM4 at values of  $5.1 \pm 0.7 \mu\text{M}$  ( $n=5$ ). In both cases, membrane currents developed independently from the rate of changes in  $[\text{Ca}^{2+}]_i$ . In cell-free inside-out patches, the concentration dependence of current activation for both channels was shifted to higher concentrations by a factor 30, but confirmed the difference in  $\text{Ca}^{2+}$  sensitivity between TRPM4 and TRPM5. Both channels revealed similar biophysical properties and are characterized by voltage-dependent activation mechanisms showing fast deactivation at negative potentials and activation at positive potentials with similar kinetics. In inside-out patches,  $\text{Ca}^{2+}$ -activated TRPM4 and TRPM5 were equally sensitive to the intracellular polyamine spermine and the antimycotic clotrimazole, while TRPM4 displayed a 10-fold higher sensitivity for block by flufenamic acid with  $\text{IC}_{50}$  of  $2.8 \mu\text{M}$  ( $n=2-8$ ) compared to TRPM5 ( $\text{IC}_{50}=24.5 \mu\text{M}$ ,  $n=6-12$ ). Importantly, we found a prominent difference in ATP-sensitivity between the channels:  $\text{ATP}^{4-}$  blocks TRPM4 with high affinity ( $\text{IC}_{50}=0.8 \pm 0.1 \mu\text{M}$ ,  $n=9-15$ ), while TRPM5 is insensitive to  $\text{ATP}^{4-}$  at concentrations up to 1 mM. In conclusion, we provide here differences between the closely related channels TRPM4 and TRPM5, which might be helpful to functionally distinguish these channels in native cells.

This work was supported by the Austrian Academy of Science, the Belgian Federal Government, the Flemish Government and the Onderzoeksraad KU Leuven.

*Where applicable, the experiments described here conform with Physiological Society ethical requirements.*

## PC73

**Potentiation of proton-gated currents in rat dorsal root ganglion neurones by arachidonic acid**

E.S. Smith, H. Cadiou and P.A. McNaughton

*Pharmacology, University of Cambridge, Cambridge, UK*

A reduction of extracellular pH activates an inward current in nociceptors (Krishtal et al. 1980). One condition associated with

tissue acidosis is inflammation, where the pH can drop to pH 5.4 (Steen et al. 1992). During the inflammatory process numerous mediators are released, including arachidonic acid (AA). It has been demonstrated that AA enhances proton-gated currents in cerebellar Purkinje neurones (Allen et al. 2002). Here we provide evidence that AA potentiates both proton-gated currents in dorsal root ganglia (DRG) neurones and the inward membrane current carried by an acid gated ion channel ASIC).

Neonatal Wistar rats (3 - 10 days old) were killed by cervical dislocation followed by decapitation. Proton-gated currents in DRG neurones and ASIC1a transfected CHO cells were examined using the whole-cell patch clamp method. Data are presented as mean  $\pm$  S.E.M.

Application of a pH 6.3 solution evoked three distinct inward currents in different DRG neurones: a slowly inactivating transient current (amplitude  $-2.57 \pm 0.4$  nA, time constant of inactivation  $2.99 \pm 0.25$  sec,  $n=52$ ), a biphasic current (rapidly inactivating transient phase =  $1.48 \pm 0.16$  nA, time constant of inactivation  $0.30 \pm 0.02$  sec, sustained phase =  $0.058 \pm 0.01$  nA,  $n=34$ ) and a pure sustained current ( $0.072 \pm 0.018$  nA,  $n=17$ ). The different inactivation times for the transient current and transient phase of the biphasic current ( $P < 0.0001$ , Student's t test) suggest different proton-gated ion channels may produce them. The sustained phase of the biphasic current has a similar amplitude to the pure sustained current suggesting the same ion channel(s) could produce them.

Addition of  $10 \mu\text{M}$  AA to the extracellular solution potentiated peak responses for all three currents: transient  $122.6 \pm 4.4$  % of control ( $P < 0.01$ , paired t test,  $n=7$ ), biphasic  $171.3 \pm 18.5$  % of control ( $P < 0.05$ ,  $n=6$ ) and sustained  $263.6 \pm 48.3$  % of control ( $P < 0.05$ ,  $n=7$ ). To investigate the contribution of ASIC1a to the potentiating effect of AA, ASIC1a was transfected into CHO cells where  $1 \mu\text{M}$  AA was found to significantly potentiate the response to pH 6.3 solution ( $288.5 \pm 43.9$  % of control,  $P < 0.01$ ,  $n=6$ ).

These data suggest that enhancement of acid mediated pain in inflammation can arise from potentiation of ASIC mediated proton-gated currents by AA. Further experiments will focus on the mechanism of action of AA.

Krishtal O. et al. (1980). *Neuroscience* 5, 2325-2327.

Steen K. et al. (1992). *J. Neurosci.* 12, 86-95.

Allen N. et al. (2002). *J. Physiol.* 543, 521-529.

This work was supported by the Medical Research Council (E. S.) and the Biotechnology and Biological Research Council (H. C.) We thank Prof. M. Lazdunski for supply of ASIC1a.

*Where applicable, the experiments described here conform with Physiological Society ethical requirements.*

## PC74

**Charged amino acids within the alpha interaction domain (AID) of Voltage-Gated Calcium Channels regulate single channel behaviour**G. Gonzalez-Gutierrez<sup>1</sup>, P. Hidalgo<sup>2</sup> and A. Neely<sup>1</sup>*<sup>1</sup>Centro de Neurociencias de Valparaiso, U. de Valparaiso, Valparaiso, Chile and <sup>2</sup>Institut für Physiologie, RWTH Aachen, Aachen, Germany*

Voltage-Dependent Calcium Channels (VDCC) are hetero-multimeres composed by at least 3 subunits: the pore forming subunit  $\alpha_1$  and auxiliary subunits  $\alpha_2/\delta$  and  $\beta$ . The  $\beta$  subunit binds to  $\alpha_1$  at

a conserved sequence of 18 amino acids in the loop joining the first a second repeat (AID; 1) In this work we show that non-conserved amino acids within the AID motif alter channel function without effect on expression. Charged amino acids in the rat CaV1.2 AID motif were either reversed or neutralized (E462R, K465N, D469S and Q473K). When co-expressed in *Xenopus* oocytes cardiac with the  $\beta_2$ -subunit ( $\beta_{2a}$ ), peak inward currents normalized by charge movement were reduced by 80 to 90% for all mutants while charge movement itself remain unchanged suggesting that regulation of expression was not affected. These mutations do not appear to prevent  $\alpha_1$ - $\beta$  interaction since voltage-dependence of activation is left-shifted by about 40 mV with co-expression of  $\beta_{2a}$ . Single channel conductance remained constant but the channel probability of being open (Po) was greatly reduced. Further studies on E462R and K465N revealed that decreases in channel Po occur through different mechanisms in each case. For E462R, repeated depolarisations (1 Hz) to 0 mV from a holding potential of -70 mV yield a large number of sweeps without channel activity ( $80 \pm 4\%$  of null sweeps for E462R compared to  $39 \pm 7\%$  found in wild type CaV1.2) while activity within active sweeps is not affected. Surprisingly, reduction in the Po by a neutralization of a Lysine three residues downs stream within AID (K465N), correlates with sweeps of activity with short burst of openings ( $1.3 \pm 0.5$  ms) without changes in the fraction of null sweeps ( $35 \pm 13\%$ ). It appears then that altering the  $\alpha_1$ - $\beta$  interaction surface as in E462R mutation, promotes a silent mode while in K465N, the low Po mode become prevalent. These results support the view that the  $\beta$  subunit regulates function by tuning dwell times among different gating modes.

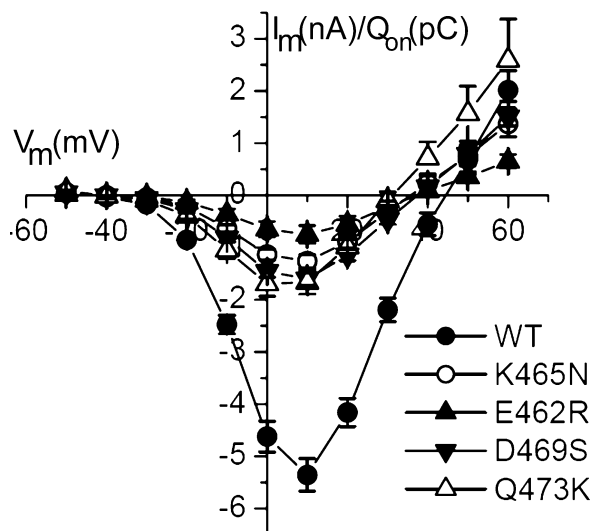


**Figure 1: IV curves for the different mutants of  $\alpha_1C$ .  $I_m$  (nA) was normalized by charge movement ( $Q_{on}$ ) and  $Q_{on}$  (pC) was measured at the onset of a depolarisation pulse to the current reversal potential (2)**

Dolphin AC. 2003. Beta subunits of voltage-gated calcium channels  
3. J Bioenerg. Biomembr. 35:599-620

Olcese R, Neely A, Qin N, Wei X, Birnbaumer L, Stefani E. 1996. Coupling between charge movement and pore opening in vertebrate neuronal  $\alpha_1E$  calcium channels. J Physiol 497:675-86

FONDECYT 1020899 to A.N. and DFG (FOR 450, TP 1) to P.H.

Where applicable, the experiments described here conform with Physiological Society ethical requirements.

PC75

### Thermodynamics of the cold receptor TRPM8

S. Brauchi<sup>1</sup>, P. Orio<sup>2</sup> and R. Latorre<sup>2</sup>

<sup>1</sup>Graduate School in Science, Universidad Austral de Chile, Valdivia, Chile and <sup>2</sup>Biophysics and Molecular Physiology, Centro de Estudios Científicos, Valdivia, Chile

The cold receptor TRPM8, also designated CMR1, is a member of the transient receptor potential, TRP, family of excitatory ion channels. TRPM8 is a channel activated by cold temperatures, voltage and cooling compounds (McKemy, *et al.* 2002). In this study we characterize the cold- and voltage-induced activation of TRPM8 channel in an attempt to identify the temperature- and voltage-dependent components involved in channel activation. Under equilibrium conditions, decreasing temperature has two effects: a) it shifts the normalized conductance vs. voltage curves towards the left, along the voltage axis. This indicates that the degree of order is higher when the channel is in the open configuration. b) It increases the maximum channel open probability, suggesting that temperature affects both voltage-dependent and voltage-independent pathways. In the temperature range between 18 to 25 °C, large changes in enthalpy ( $\Delta H = -112$  kcal/mol) and entropy ( $\Delta S = -384$  cal/mol °K) accompany the activation process ( $n=9$ ). The  $Q_{10}$  calculated in the same temperature range is 23 ( $n=9$ ). This thermodynamic analysis strongly suggests that the process of opening involves large conformational changes of the channel-forming protein. The highly temperature-dependent transition between open and closed configurations is thus possible because enthalpy and entropy are both large and compensate each other. Our results indicate that neither temperature nor voltage are strictly necessary for TRPM8 channel activation and that they can be understood in an allosteric voltage- and temperature-gating kinetic scheme.

McKemy D.D., *et al.* (2002) J.Neurosci. 22, 6408-6414

S.B. is recipient of a CONICYT doctoral fellowship. R.L. was supported by Chilean grant FONDECYT 103-0830. CECS is a Millennium Institute and is funded in part by a grant from Fundación Andes.

Where applicable, the experiments described here conform with Physiological Society ethical requirements.

PC76

### Epithelial growth factor impairs functional expression of the amiloride-sensitive sodium channel in cystic fibrosis cells

L. Cao<sup>1</sup>, G. Owsianik<sup>1</sup>, F. Becq<sup>2</sup> and B. Nilius<sup>1</sup>

<sup>1</sup>Department of Physiology, Catholic University of Leuven, Leuven, Belgium and <sup>2</sup>Institut de Physiologie et Biologie Cellulaires CNRS UMR 6187, Université de Poitiers, Poitiers, France

ENaC is a heteromultimeric channel composed of 3 homologous subunits,  $\alpha$ -,  $\beta$ - and  $\gamma$ -ENaC. It mediates the electrogenic  $Na^+$  transport across the apical membrane. The regulation of ENaC function is complex and involves various hormones such as aldosterone, vasopressin, insulin as well as



epithelial growth factor (EGF). The acute mode of EGF-dependent inhibition of ENaC-mediated  $\text{Na}^+$  absorption is presumably by means of an increase in intracellular calcium and/or through the extracellular signal-regulated protein kinase (ERK) signaling pathway. The molecular mechanisms of long-term EGF-mediated regulation of ENaC function are not well known yet.

To investigate the effects of the long-term application of EGF on ENaC function, we used a cystic fibrosis (CF) cell line, JME/CF15, derived from a nasal epithelium of a CF patient. Using the whole-cell mode of the patch-clamp technique, we measured an amiloride-sensitive  $\text{Na}^+$  current ( $2.0 \pm 0.5$  pA/pF at  $-100$  mV;  $n=13$ ) in cells growing in the EGF-free medium. This current was only observed in 1/3 of measured cells. The reversal potential of this current was dependent on  $\text{Na}^+$  concentrations and the cation selectivity was much higher for  $\text{Na}^+$  than for  $\text{K}^+$ . These results indicate that the observed amiloride-sensitive  $\text{Na}^+$  current in JME/CF15 cells is most likely through ENaC channels. In contrast to cells growing in EGF-free conditions, cells growing in the EGF-containing medium did not show any amiloride-sensitive  $\text{Na}^+$  currents. This effect was transient, since amiloride-sensitive  $\text{Na}^+$  currents were measured again when the cells were shifted back to the EGF-free medium. Immunocytochemical experiments with specific anti- $\alpha\text{ENaC}$  antibodies in permeabilized JME/CF15 cells showed that in cells cultured in EGF-containing medium  $\alpha\text{ENaC}$  was mainly detected in a region around the nucleus, most likely in the endoplasmic reticulum (ER), while in cells growing in the EGF-free medium  $\alpha\text{ENaC}$  signals were more distributed over the cell body. In addition, the western blotting analysis of the whole cell extract from cells growing in the presence of EGF showed 2-fold increase of non-glycosylated and the absence of glycosylated  $\alpha\text{ENaC}$  fractions when compared to cells from the EGF-free culture. Taken together our data show that in JME/CF15 cells, the ENaC channel function is completely inhibited by the long-term incubation with EGF most likely as an effect of impaired trafficking and surface expression of ENaC channels.

Supported by the EC grant: CF-PRONET (QLG1-CT-2001-01005).

Where applicable, the experiments described here conform with Physiological Society ethical requirements.

---

PC77

### Molecular determinants in the activation of heag potassium channels

M. Ju and D. Wray

Biomedical Sciences, Leeds University, Leeds, UK

Heag1 and heag2 channels are members of the eag family of human potassium channels. These channels have high sequence similarity, but differ in their electrophysiological properties, such as steady state activation (Ju & Wray, 2002). In this study, we have investigated the molecular regions that contribute to the differences in steady state activation between heag1 and heag2 channels, focussing here on which parts of the membrane-spanning regions S1 to S6 are involved. One might expect

that differences in activation are due to the voltage sensor region S1-S4.

For this, chimeras between heag1 and heag2 were constructed by restriction digest and subsequent ligation, transferring corresponding regions between the channels. The chimeras were expressed in *Xenopus* oocytes and currents were recorded two days later at room temperature. Oocytes were depolarized from a holding potential of  $-80$  mV to test potentials from  $-70$  mV to  $+70$  mV. Conductance-voltage (G-V) curves were obtained and fitted to the Boltzmann equation. Controls with wild type channels were used in the same batch of oocytes as the chimeras.

Chimera I had the S1 to S6 transmembrane region of heag2 (residues 138-549) replaced by heag1. For this chimera, the Boltzmann slope parameter  $k$  was similar to that for wild type heag1 channel, but significantly different from that for wild type heag2 channel (chimera I:  $13.7 \pm 1.0$  mV,  $n=8$ ; wild type heag2:  $42.0 \pm 3.1$  mV,  $n=4$ ,  $P<0.05$ , Student's unpaired t-test). This confirms that indeed as expected, the S1-S6 region is involved in determining steady state activation in heag channels.

To determine which parts of the S1-S6 region are involved, we studied further constructs. Chimera II had the S1 to S4 transmembrane region of heag2 (residues 138-331) replaced by heag1. The slope parameter  $k$  for this chimera was intermediate in magnitude between wild types heag1 and heag2; for the chimera,  $k$  was  $32.9 \pm 1.5$  mV,  $n=8$ , a value significantly different ( $P<0.05$ ) from both wild type heag1 ( $23.3 \pm 1.4$  mV,  $n=7$ ) and heag2 ( $50.0 \pm 3.8$  mV,  $n=8$ ). Chimera III, with the S5 to S6 region of heag2 (residues 332-549) replaced by heag1 showed a  $k$  value ( $13.5 \pm 0.8$  mV,  $n=8$ ) that was closest to, but not identical to, that for heag1 ( $23.2 \pm 1.0$  mV,  $n=7$ ) rather than heag2 ( $40.4 \pm 2.5$  mV,  $n=7$ ).

Taken together, the data show that, residues within the whole of the S1-S6 transmembrane region are involved in determining differences in steady state activation between heag1 and heag2 channels; both S1-S4 and S5-S6 regions are involved in the effect. Thus it is not only the voltage sensor, but also the pore region that determines voltage sensitivity of activation.

M. Ju & D. Wray (2002), FEBS Lett, 524, 204-210.

Supported by BBSRC

Where applicable, the experiments described here conform with Physiological Society ethical requirements.

---

PC78

### FUNCTIONAL INTERACTION BETWEEN ANNEXINS AND MAXI-CHLORIDE CHANNEL IN HUMAN PLACENTA

P. Llanos<sup>1</sup>, B. Campos<sup>2</sup> and G. Riquelme<sup>1</sup>

<sup>1</sup>Inst. Ciencias Biomedicas, Facultad de Medicina, Universidad de Chile, Santiago, Chile and <sup>2</sup>College of Medicine, University of Cincinnati, Cincinnati, OH, USA

The human syncytiotrophoblast acts as the principal physiological barrier between foetal and maternal blood. In this epithelium, functions such as maintenance of membrane voltage, solute transport and cell volume regulation, involve chloride currents. A major contributor to these currents is a Maxi-chloride channel present in the apical syncytiotrophoblast membrane. Diverse studies have demonstrated the modulation of other chloride

channels by annexins, proteins that bind to acidic phospholipid membranes in a calcium-dependent manner. Within the family of the annexins, one of the most abundant members in syncytiotrophoblast is annexin VI; although various functions have been attributed to annexin VI, its precise physiological role in placenta has yet to be defined. The purpose of this study was to evaluate the effects of annexin VI on the biophysical properties of the Maxi-chloride channel present in apical syncytiotrophoblast membrane from human placenta.

Using isolated membranes prepared from term placental tissue through a protocol that includes differential centrifugation, precipitation with magnesium chloride and discontinuous sucrose gradient, and reconstituted into giant liposomes suitable for Patch-clamp recording of single channels, we have previously characterised the apical membrane Maxi-chloride channel: multiple substates, major substate conductance of 240 pS, voltage dependent open probability (being open between  $\pm 50$  mV and closing at more extremes potentials), permeability to diverse anions (including amino acids), direct inhibition by arachidonic acid, steroid hormones and DIDS.

The presence of annexin VI was detected in both sections of placental villi tissue and purified apical plasma membrane, using immunohistochemistry and western blot analysis with polyclonal anti-annexin VI antibody. Addition of 5  $\mu$ g/ml anti-annexin VI antibody in the bath solution of electrophysiological patch-clamp experiments induced a decrease in both the total chloride current ( $39 \pm 1.9\%$  decrease;  $n=4$ ) and the Maxi-chloride major substate single channel conductance ( $105 \pm 13$  pS;  $n=4$ ). The anti-annexin VI antibody also induced marked flattening of the open probability versus voltage curve, suggesting a loss of voltage dependence of open probability of the Maxi-chloride channel. The addition of a preimmune serum did not induce significant changes in the mentioned variables with respect to values in control conditions. Our results suggest that the endogenous annexin VI of human syncytiotrophoblast regulates the Maxi-chloride channel of apical membrane. The modulation of these channels by annexin may be of great importance in placental physiology and pathophysiology.

FONDECYT-CHILE 1040546

Where applicable, the experiments described here conform with Physiological Society ethical requirements.

PC79

### Copper: an endogenous modulator of neuronal excitability?

C. Vergara<sup>1</sup>, F. Aedo<sup>1</sup>, R. Delgado<sup>2</sup> and D. Wolff<sup>1</sup>

<sup>1</sup>University of Chile, Santiago, Chile and <sup>2</sup>Millennium Institute CBB, Santiago, Chile

The idea that synaptically released copper affects the excitability of cells around the release site has been proposed based on several indirect evidences: a) uneven distribution of copper, generally co-stored with zinc, in synaptic vesicles in different zones of the central nervous system (CNS), b) neurological symptoms of patients of Menkes and Wilson diseases, whose copper levels in the CNS are decreased or increased respectively and c) reports that several neurotransmitter activated currents are

blocked by nano to micro molar copper concentration in vitro (1).

We started a direct characterization of the effect of  $\text{Cu}^{++}$  upon neuronal excitability using olfactory neurons from the toad *C. caudiververa* as model cells. The olfactory epithelia was obtained from animals killed after ice immersion, a procedure authorized by the University of Chile Ethics Committee. These cells present a TTX sensitive  $\text{Na}^+$  current ( $I_{\text{Na}}$ ), a non inactivating  $\text{Ca}^{++}$  current ( $I_{\text{Ca}}$ ), a delayed rectifier  $\text{K}^+$  current ( $I_{\text{K}}$ ) and a  $\text{Ca}^{++}$  activated  $\text{K}^+$  current ( $I_{\text{Ca-K}}$ ). The effect of  $[\text{Cu}^{++}]$  upon each current was determined under voltage clamp in the whole cell configuration. Micromolar  $\text{Cu}^{++}$  (1 - 10) caused a dose dependent block of  $I_{\text{Na}}$  and also of  $I_{\text{Ca}}$ . As a consequence,  $I_{\text{Ca-K}}$  was reduced but  $I_{\text{K}}$  was basically not affected. The neuronal firing rate induced by depolarizing current pulses was decreased by copper in this concentration range. Copper in the nanomolar range (10 - 100) caused an increase in the amplitude of  $I_{\text{Na}}$  due to an increase in the activation and inactivation rates and it did not appreciably affect the other 3 currents. An increase of  $I_{\text{Na}}$  activation rate hints that in these conditions neurons could be more excitable. Indeed, the firing rate induced by depolarizing current pulses was increased by 10-50 nM  $\text{Cu}^{++}$ . The spontaneous firing rate of groups of cells in the whole undissociated epithelia recorded extracellularly increased and then decreased when exposed to nanomolar followed by micromolar copper (4.2 fold  $\pm$  2.3 SD increase by 50 nM  $\text{Cu}^{++}$ , 2.9 fold  $\pm$  1.3 SD decrease by 5  $\mu$ M  $\text{Cu}^{++}$ ;  $n=4$ ). Since  $\text{Cu}^{++}$  is generally co-liberated with  $\text{Zn}^{++}$  we also tested its effect upon  $I_{\text{Na}}$ . Nanomolar  $\text{Zn}^{++}$  also activates  $I_{\text{Na}}$  but the blockade of this current by micromolar  $\text{Zn}^{++}$  is less effective (100  $\mu$ M blocked only 25% of  $I_{\text{Na}}$ ). The activating effect of nanomolar copper was not reverted by washing it from the solution nor by adding chelators but 2 mM of the reducing agent DTT reversibly modulated the basal firing rate. We propose that at least part of the effect of  $\text{Cu}^{++}$  upon excitability is redox-mediated. These results directly support a role for copper as modulator of neuronal excitability.

Horning MS & Trombley PQ (2001) *J. Neurophysiol.* **86**, 1652-1660.

Financed by: ICA-CIMM, Fondecyt 1040681.

Where applicable, the experiments described here conform with Physiological Society ethical requirements.

PC80

### Abolition of gating in ClC-2 by a double mutation affecting pore and CBS domains.

L. Zuniga, M. Catalan, A. Cardenas, L. Cid and F. Sepulveda

Centro de Estudios Científicos, Valdivia, Chile

Functional and structural studies demonstrate that  $\text{Cl}^-$  channels of the ClC family have a dimeric double-barrelled structure, with each monomer contributing an identical pore. We have recently provided evidence for the presence of slow and fast hyperpolarisation-dependent gating processes in ClC-2 that might correspond to protopore gating and common process opening both pores simultaneously. Unlike the case with ClC-0, the prototype ClC  $\text{Cl}^-$  channel, the two gating processes in ClC-2 are not independent (Niemeyer et al., 2003; Zúñiga et al., 2004). Recently the role of C-terminus CBS domains in the common

gating process of ClC-0 and ClC-1 has been demonstrated (Estevez et al., 2004), with a single-point mutation abolishing this gate. There is a high degree of conservation of CBS domains in ClC-2 and we have now examined the effect of the mutating the corresponding amino acid (H811) on ClC-2 gating. We have used the recombinant guinea pig ClC-2 transiently expressed in HEK-293 cells and assayed by the whole-cell recording mode of the patch-clamp technique. The H811A mutant of ClC-2 is seen to conserve the strict inward rectification of the WT channel, but with a much faster kinetics for opening and closing. The overall kinetics is still bi-exponential but the time constants are decreased two-fold in the mutant. The voltage-dependence of H811A is shifted to more positive potentials by about 30 mV.  $\text{Cd}^{2+}$  is known to block ClC channels purportedly by facilitating slow closing. However,  $\text{Cd}^{2+}$  inhibited to same extent and affinity both WT and H811A channels. Interestingly the intracellular  $\text{Cl}^-$  dependence is not affected by the mutation.  $V_{0.5}$  is related linearly to  $\log[\text{Cl}^-]_i$  with similar slope in H811A and WT channels. Neutralisation of a conserved pore glutamic acid residue (E217) has been shown to abolish all  $\text{Cl}^-$  dependence in ClC-2 (Niemeyer et al., 2003). This mutant retains, however, a residual voltage-dependence that has been attributed to slow, common gate. The double mutant E217V-H811A is a constitutive open channel completely lacking any gating. We conclude that, if ClC-2 has both fast and slow gating processes, akin to the protopore and common gates of other ClC channels, these two processes must be highly coupled.

Estevez, R., Pusch, M., Ferrer-Costa, C., Orozco, M., & Jentsch, T. J. (2004). *J. Physiol. (London)* 557, 363-378

Niemeyer, M. I., Cid, L. P., Zuñiga, L., Catalan, M., & Sepulveda, F. V. (2003). *J. Physiol. (London)* 553, 873-879.

Zuñiga, L., Niemeyer, M. I., Varela, D., Catalan, M., Cid, L. P., & Sepulveda, F. V. (2004). *J. Physiol* 555, 671-682.

Fondecyt 1030627 and 1020652. L.Z. is a Universidad Austral de Chile PhD student.

Where applicable, the experiments described here conform with Physiological Society ethical requirements.

---

PC82

## INHIBITION OF CELL PROLIFERATION AND INDUCTION OF APOPTOSIS IN *Trypanosoma cruzi* BY SESQUITERPENE LACTONES: POSSIBLE ROLE OF THE POTASSIUM CONDUCTANCES

V. Jimenez<sup>1</sup>, R. Paredes<sup>1</sup>, M. Sosa<sup>2</sup>, G. Riquelme<sup>1</sup> and N. Galanti<sup>1</sup>

<sup>1</sup>Faculty of Medicine- University of Chile, Santiago, Chile and

<sup>2</sup>IHEM, Faculty of Medical Sciences, UNCuyo, Mendoza, Argentina

*Trypanosoma cruzi*, the agent of Chagas' disease, is a parasitic protozoan which presents three cellular forms during its life cycle: epimastigote (extracellular and replicative form in the vector hematophagous insect), amastigote (intracellular and replicative form in mammals) and trypomastigote (extracellular non-replicative form in mammals).

Sesquiterpene lactones are a group of natural compounds characterized by the presence of a  $\gamma$ -lactone ring and a  $\alpha$ -methylene group, displaying diverse biological effects, such as antitumoral and antimicrobial. In this study we have evaluated the effect of

two sesquiterpene lactones, dehydroleucodine (DhL) and heheline (HLN), on *T. cruzi* epimastigotes.

Both compounds inhibit DNA synthesis and reduce protein synthesis, thus clearly affecting cell proliferation (thymidine and leucine-tritiated incorporation means in treated epimastigotes 64.5% and 3.5% respectively, as percentage of control). Additionally, they induce apoptosis as measured by TUNEL (treated  $65.4 \pm 11.4\%$  vs control  $4.1 \pm 1.3\%$ ), and increase the immunoreactivity of caspases 3 and 8, as detected by immuno-western blot (Laemmli, 1970).

Apoptosis is a process of cell death in which the cell undergoes nuclear and cytoplasmic shrinkage, chromatin condensation, nuclear fractionation, dissipation of transmembrane and mitochondrial potential and finally the disruption of plasma membrane. Among other cations, changes in  $\text{K}^+$  homeostasis are known to lead to the loss of plasma membrane potential.

In order to establish the role of potassium plasma membrane conductances in the apoptosis induction process, we have isolated, by differential centrifugation, plasma membranes of *T. cruzi* epimastigotes (Benaïm et al. 1991). The purified membranes were reconstituted in giant liposomes (Riquelme et al. 1990) and their electrophysiological activities were registered by patch-clamp technique (Hamill et al. 1981). This is the first and preliminary approximation to the nature and role of ionic conductance in *T. cruzi*.

Our evidences point to a possible antiproliferative and proapoptotic action of DhL and HLN on *T. cruzi* at different cellular levels, and open new pharmacological perspectives for the control of the parasite.

Laemmli, U.K. (1970). *Nature* 227, 680-685.

Benaïm, G., Losada, S., Gadelha, F.R., and Docampo, R. (1991). *Biochem. J.* 280, 715-720.

Riquelme, G., Lopez, E., Garcia-Segura, L.M., Ferragut, J.A., and Gonzalez-Ros, J.M. (1990). *Biochemistry* 29, 11215-11222.

Hamill, O.P., Marty, A., Neher, E., Sakmann, B., and Sigworth, F.J. (1981). *Pflügers Arch.* 391, 85-100.

CONICET- Argentina, Fondecyt grant 1040546, Chile and SIDA/SAREC Network for Research and Training in Parasitic Diseases.

Where applicable, the experiments described here conform with Physiological Society ethical requirements.

---

PC83

## Critical role of extracellular histidines for copper and zinc modulation of P2X<sub>2</sub> receptor

R.A. Lorca<sup>1</sup>, C. Arredondo<sup>2</sup>, P. Bull<sup>2</sup> and J. Huidobro-Toro<sup>1</sup>

<sup>1</sup>Department of Physiology, P. Catholic University of Chile, Santiago, Chile and <sup>2</sup>Department of Molecular Genetics and Microbiology, P. Catholic University of Chile, Santiago, Chile

The P2X receptors are widely expressed in CNS and other tissues. ATP-evoked currents in P2X<sub>2</sub> receptor are potentiated by 1-300  $\mu\text{M}$  copper or zinc; this receptor possesses nine extracellular histidines, two of which, H120 and H213, were reported to be involved in the zinc-induced potentiation (Clyne et al. 2002). However it remains unknown which of the extracellular his-

tidines are necessary for the copper-induced potentiation. This study was aimed to determining whether the same extracellular histidines are also critical for copper action, suggesting a common metal coordination site and similar mechanisms of potentiation of the P2X<sub>2</sub> receptor.

Wild-type (wt) P2X<sub>2</sub> receptors and nine single amino acid site-directed mutants in which histidines were replaced by alanines, were expressed in *Xenopus laevis* oocytes. We used the two electrode voltage-clamp technique to study the copper and zinc-induced potentiation of the ATP-evoked currents. ATP was applied for 10 sec; ATP concentration-response curve protocols were performed in wt as well as the mutant receptors. In addition, trace metal concentration-response curves were performed using 10 μM ATP in wt or the mutant receptors.

The ATP EC<sub>50</sub> in wt receptors, derived from concentration-response curves, was 33.3±2.5 (n=30), 10 μM copper or zinc preincubated for 1 min potentiated the ATP-evoked currents and reduced the ATP EC<sub>50</sub> (4.3±0.9 and 16.8±2.7 respectively, p<0.01, Kruskal-Wallis test). The 10 μM ATP-evoked current was potentiated by 10 μM copper or zinc (28±5.9 and 6.2±1-fold). In the H120A, H213A or H245A mutants we consistently observed that 10 μM copper or zinc did not potentiate the ATP-evoked currents, neither changed the ATP EC<sub>50</sub>. However, in the H192A and H319A mutants, the magnitude of the 10 μM copper or zinc potentiation was diminished in comparison with the wt receptor, but these metals still potentiated the ATP-gated currents (3-10 fold for copper, and 3-4 fold for zinc). The other mutants examined (H125A, H146A, H152A and H174A) demonstrated that these metals potentiated the ATP responses similarly to the wt receptors.

These results suggest that copper and zinc interact at a common binding-site composed of three critical histidines (H120, H213 and H245) plus two accessory histidines (H192 and H319). We conclude that the identified histidine residues conform the metal-binding site which coordinate trace metals causing a conformational change responsible for the observed increase in the ATP-gated currents.

Clyne J.D., LaPointe L.D. and Hume R.I. (2002) *J Physiol* **539**: 347-359.

Funded by FONDAP 13980001, MIFAB and ICA grants.

Where applicable, the experiments described here conform with Physiological Society ethical requirements.

## PC84

### Identification of critical amino acids of the regulatory binding-sites for trace metals in the P2X<sub>4</sub> receptor.

C. Coddou, C. Arredondo, P. Bull and J. Huidobro-Toro

*Department of Physiology, P. Catholic University, Santiago, Chile*

P2X receptors are ligand-gated ionic channels, and can be differentially modulated by divalent metals that bind to specific allosteric sites. We previously demonstrated that His-140 is a critical amino acid responsible for the inhibitory modulation exerted by copper on the P2X<sub>4</sub> receptor, and the facilitatory action of zinc is augmented and its typical modulation, a bell-shaped curve observed in the wild-type receptor is replaced by a sigmoid in this mutant, suggesting that zinc can bind to the inhibitory site too at high concentrations (Coddou et al., 2003).

Since metal coordination requires more than one amino acid, we replaced other amino acids in the vicinity of His-140 that could form part of the inhibitory binding site and the mutated cDNAs were injected in *X. laevis* oocytes and tested with electrophysiological techniques. We found that the replacement of Asp-138 by an alanine (D138A) results in a loss of copper-induced inhibition (with no inhibition of ATP-evoked currents with 10 μM Cu<sup>2+</sup> and a 47.6±15.5% inhibition with 300 μM Cu<sup>2+</sup>) and an increase of the zinc-induced potentiation (20.1±2.4 fold increase) much similar to that observed in the H140A mutant. However mercury still inhibited the ATP-evoked currents in this mutant with an IC<sub>50</sub> of 3.7±1.3 μM (n=4), suggesting that this metal exerts its effects by a different site of copper. Asp-129 had a modest contribution of copper-induced inhibition, with an IC<sub>50</sub> of 24.9±4.4 μM (n=4), whereas the zinc-induced potentiation was diminished. The D131A mutant showed no significant differences with wild type receptor on the inhibitory action of copper and a slightly increase in zinc-induced potentiation. It has been suggested a key role of Cys-132 for zinc facilitation (Xiong et al., 2003), but no other amino acids responsible for metal facilitation has been identified. In the C132A mutant the zinc-induced potentiation was completely lost and zinc inhibited the ATP-evoked currents. The copper-induced inhibition was also augmented in this mutant with an IC<sub>50</sub> of 1.5±0.9 μM (n=3). These results show that both Asp-138 and His-140 are critical for the inhibitory action of copper, zinc and cadmium and form part of the inhibitory binding-site of the P2X<sub>4</sub> receptor. On the other hand, Cys-132 is part of the facilitatory-site that coordinates zinc and/or cadmium. The role of Asp-129 seems to be minor contributing modestly to the binding of metals to both the inhibitory and facilitatory sites.

Coddou C, Morales B, Gonzalez J, Grauso M, Gordillo F, Bull P, Rassen-dren F, Huidobro-Toro JP. *J Biol Chem.* (2003) 278:36777-85.

Xiong K, Stewart RR, Peoples RW, Weight FF, Li C. Poster E66, SFN 33rd Annual Meeting, New Orleans, LA, USA, 2003.

Funded by FONDAP 13980001, MIFAB and ICA grants.

Where applicable, the experiments described here conform with Physiological Society ethical requirements.

## PC85

### Chloride movement through lateral membrane of apical outer hair cells in isolated cochlear coils of the guinea pig

J. Ashmore and J. Mikiel-Hunter

*Physiology, UCL, London, UK*

In the mammalian inner ear, outer hair cells (OHCs) control mechanics of the cochlear partition. They do so through their electromotility, a property where cells generate longitudinal forces exerted by a motor protein named prestin (SLC26A5), in the cells lateral membrane. It has been proposed that prestin acts as an incomplete anion transporter (Oliver et al, 2001). To study this possibility further we have investigated how OHC currents respond to anion replacement.

We used a novel preparation in which coils of the organ of Corti (approximately half a turn) were imaged without further dissection. Coils were dissected from the cochlea of adult guinea-pigs humanely killed according to a Schedule 1 protocol. The

coils were dissected on ice and held by a fine mesh grid on the stage of an upright microscope under temperature control. Identified OHCs were recorded under tight-seal whole-cell conditions for greater than 40 minutes with little deterioration. The recording patch pipettes containing (in mM): K, 140; EGTA 0.5; Mg 2; Cl 144; Hepes 10; (adjusted to pH 7.3 and 320 mOsm). The extracellular solution contained: Na 140; K 4; Cl 150; Ca 1; Mg 2; Hepes 10, pH 7.3 and matching osmotic strength. Where necessary chloride was replaced with gluconate and solutions were exchanged by continuous perfusion of the chamber.

Cells from the cochlear apical turn exhibited a nonlinear I-V curve with outward rectification prominent above -20mV. The OHC input slope conductance at -50 mV was  $10.3 \pm 1.8$  nS (s.e.m., n=16; range 1.6-16.6 nS) whereas at +30 mV the slope increased by a mean factor of 2.12. Reduction of external chloride reduced the outward current at +30mV by approximately 50%. Application of 1 mM 4-AP, proposed to block IK in apical OHCs (Mammano & Ashmore, 1996), did not remove the effect of low external chloride. A tail current analysis suggested that outward current at depolarised levels was a result of a significant chloride movement through the membrane although the replacing anion, gluconate, was partially permeable. A similar permeability was found for sulfamate. Lowering intracellular chloride to 30 mM and to 1 mM in the pipette reduced outward current, the effect of then lowering external chloride remaining in accordance with modified GHK equation predictions. The simplest model which explains the present data is one where significant chloride movement occurs through prestin, a transporter with a chloride-activated gate at both external and cytoplasmic sites. The high density of prestin ( $>10^7$  copies / cell) in the OHC lateral membrane provides an opportunity to measure these currents.

Mammano, F & Ashmore, J. F. (1996). *J. Physiol.* 496:639-646.

Oliver, D. et al., (2001). *Science*. 292:2340-3

Supported by the Wellcome Trust. JMH held a Physiological Society Vacation studentship

*Where applicable, the experiments described here conform with Physiological Society ethical requirements.*

---

## PC86

### Changes in morphological and physiological properties in dissociated adult skeletal muscle fibers of rat in vitro

H. Talarmin, J.P. Pennec, M. Droguet, J. Morel, S. Talon, M. Metges, M. Gioux and G. Dorange

EA 3879 / I3S, Brest, France

The aim of this study was to establish a co-culture model of rodent neurons, striated muscle fibres and glial cells, in order to get a better understanding of nerve-muscle interactions. The first step was to determine the evolution of morphological and physiological properties of isolated adult rat flexor digitorum brevis muscle fibres maintained in vitro under various culture conditions: cultured alone or co-cultured, cultured on a substrate uncoated or coated with an extracellular matrix (Matrigel). Voltage-gated sodium channels (NaChs) and acetylcholine receptors (AChRs) were characterized using the patch-clamp technique or

by cytochemistry. When the fibres were cultured for up to 3 weeks alone in suspension in DMEM supplemented with 10% fetal calf serum (FCS), clusters of AChRs and NaChs normally located in the postsynaptic membrane of striated fibres gradually disappeared from the synaptic region after 7 days under these culture conditions. Simultaneously, Na<sup>+</sup> currents decreased at the endplate area and increased along the fibre as revealed by patch clamp. Fibres cultured on Matrigel in a medium supplemented with 10% FCS showed lower survival duration (10 days). After 4-5 days culture, fibroblastic cells proliferated. The major part of these cells (around 60%), positive for anti-desmin and/or anti-vimentin, were satellite cells. Other adherent cells were fibroblasts (only positive for anti-vimentin) and probably endothelial cells. The reduced survival of adult fibres in vitro was believed to be related to the proliferative activity of satellite cells. Patch clamp and/or cytochemistry showed that AChRs and NaChs remained clustered at the endplate area in the fibres cultured on Matrigel (at least up to 6 days). However, an increase in sodium currents was also observed along the fibre. In co-culture, the Na<sup>+</sup> conductance, recorded from patches situated far from the endplate of fibres co-cultured with neurons isolated from the dorsal portion of the spinal cord of newborn rats, increased from  $4.78 \pm 0.86$  nA V<sup>-1</sup> at D2 to  $9.71 \pm 2.91$  nA V<sup>-1</sup> at D6 ( $P < 0.05$ , Mann-Witney test). The D6 value was not significantly different ( $P > 0.05$ ) from the value found in suspended fibres ( $9.38 \pm 1.97$  nA V<sup>-1</sup>) at the same culture duration. Now, the control value measured in co-culture at D2 was lower than the value observed in fibres of the same culture duration cultured in suspension ( $6.46 \pm 1.07$  nA V<sup>-1</sup>) or on extracellular matrix ( $6.05 \pm 2.46$  nA V<sup>-1</sup>); this was attributed to the effects of nervous released factors. Na<sup>+</sup> currents increased at D6 when compared with D2 values in all conditions. These findings were consistent with the hypothesis of a neosynthesis of Na<sup>+</sup> channels in isolated fibres, correlated with a decrease of channel density at the endplate especially in DMEM cultured fibres. The increase in the time constants of the Na<sup>+</sup> current observed in co-culture is related to a greater increase in the population of TTX-resistant Na<sup>+</sup> channels.

*Where applicable, the experiments described here conform with Physiological Society ethical requirements.*

---

## PC87

### Exogenous phosphatidylinositol-3,4,5-trisphosphate (PIP3) induced platelet activation and cation entry; studies of PIP3 on transiently expressed TRPC6.

S. Hassock, S. Ayman and K. Authi

King's College London, London, UK

Recent studies in platelets and T-cells have reported the involvement of phosphoinositide-3-kinase (PI-3-K) in calcium entry that is independent of regulation by intracellular stores. A cell permeable analogue of PIP3 namely dioctanoyl-PIP3 (DiC8-PIP3) induces cation entry in both T-cells and platelets. DiC8-PIP3 induces platelet aggregation though the full mechanisms are not established. Platelets express the transient receptor potential canonical (TRPC)1 and TRPC6 cation channels and we have suggested TRPC6 to be the major non-store regulated

channel. TRPC6 also contains a p85 PI-3-K recognition motif. In this study we investigated a possible link between DiC8-PIP3 and TRPC6.

Platelet aggregation and  $\text{Ca}^{2+}$  elevation were carried out using standard techniques. Akt activation was estimated using Western blotting. Transient transfection of desired proteins was carried out in QBI-293 cells using 30–60  $\mu\text{g}$  of plasmid DNA to 70% confluent cells using the standard calcium phosphate technique. After 24 hrs cells were provided with fresh medium and experiments carried out 48 hrs later after labelling of cells with Fura2. Cytosolic calcium levels were monitored using 340/380 nm ratio fluorescence measurements.

DiC8-PIP3 induces platelet aggregation with similar potency in either  $\text{Ca}^{2+}$  or  $\text{Ba}^{2+}$  containing medium and induces  $\text{Ca}^{2+}$  or  $\text{Ba}^{2+}$  entry without release from intracellular stores. DiC8-PIP3 also induced the activation of Akt in platelets as determined using an anti-phospho-Akt antibody suggesting that it activates other PIP3 effectors. Studies on hTRPC6 was carried out in QBI-293 cells. Fura2 loaded QBI-293 cells show typical responses of  $\text{Ca}^{2+}$  release and  $\text{Ca}^{2+}$  entry in response to carbachol addition and there was no response of  $\text{Ca}^{2+}$  elevation when the diacylglycerol analogue OAG was added. Over-expression of hTRPC6 resulted in an increase of OAG induced entry of  $\text{Ca}^{2+}$  /  $\text{Ba}^{2+}$  signifying the properties of over-expressed hTRPC6. Western blotting using anti-TRPC6 antibodies confirmed the over-expression. Stimulation of hTRPC6 cells with DiC8-PIP3 (20  $\mu\text{M}$ ) did not induce  $\text{Ca}^{2+}$  elevation suggesting the absence of a direct effect on hTRPC6. A recent study has suggested that TRPC6 can be tyrosine phosphorylated leading to positive modulation of channel activity. However co-expression of either hSYK or hFYN did not result in any stimulation of  $\text{Ca}^{2+}$  elevation with DiC8-PIP3 whilst the response to OAG was maintained. These results suggest that the non-store regulated, DiC8-PIP3 stimulation of cation entry in platelets most likely results from an indirect stimulation of cation entry channels via other PIP3 effectors.

This work is supported by the British Heart Foundation.

Where applicable, the experiments described here conform with Physiological Society ethical requirements.

## PC88

### Characterization of $\text{Ca}^{2+}$ -dependent $\text{K}^{+}$ channels from rat olfactory cilia incorporated into planar lipid bilayers

K. Castillo<sup>1</sup>, J. Bacigalupo<sup>1</sup> and D. Wolff<sup>1</sup>

<sup>1</sup>Biology, University of Chile, Faculty of Sciences, Santiago, Metropolitan, Chile and <sup>2</sup>Millennium Institute CBB, Santiago, Chile

In olfactory receptor neurons, odorants elicit excitatory and inhibitory responses, associated to an increase and to a decrease in the action potential frequency, respectively. The inhibitory response involves the opening of cyclic nucleotide gated channels via the cyclic AMP cascade that leads to activation of  $\text{Ca}^{2+}$ -dependent  $\text{K}^{+}$  ( $\text{K}_{\text{Ca}}$ ) channels. Patch-clamp studies performed in our laboratory demonstrated the presence of low, intermediate and high conductance  $\text{K}_{\text{Ca}}$  channels in the olfactory cilia (Delgado et al., 2003). In the present study, we carried out the biophysical and pharmacological characterization of these ciliary

$\text{K}_{\text{Ca}}$  channels. This was addressed by studying the  $\text{K}_{\text{Ca}}$  channels from a purified rat olfactory cilia membrane fraction, incorporated into planar phospholipid bilayers. Olfactory tissue was obtained from adult rats sacrificed with anaesthesia overdose (pentobarbitone 60 mg/Kg), according with the guidelines of the Ethics Committee of the University of Chile. Data are expressed as mean  $\pm$  S. D. Low (S), intermediate (I) and high (B) conductance  $\text{K}_{\text{Ca}}$  channels, were incorporated into the bilayers, in symmetrical 100 mM  $\text{K}^{+}$ . The  $\text{SK}_{\text{Ca}}$  channel showed a  $16.3 \pm 0.7$  pS ( $n = 6$ ) conductance, insensitivity to voltage, and sensitivity to  $\text{Ca}^{2+}$  ( $K_{0.5} = 57.1 \pm 2.1$   $\mu\text{M}$ ,  $n = 3$ ) and to apamin. We identified two different  $\text{IK}_{\text{Ca}}$  channels. One presented two open conductance levels, of  $30.3 \pm 1.4$  pS and  $50.5 \pm 1.9$  pS ( $n = 7$ ), was sensitive to  $\text{Ca}^{2+}$  ( $K_{0.5} = 59.8 \pm 0.9$   $\mu\text{M}$ ,  $n = 2$ ), clotrimazole and insensitive to voltage and to charybdotoxin. The other  $\text{IK}_{\text{Ca}}$  channel showed an open conductance of  $59.6 \pm 1.4$  pS ( $n = 5$ ) and was sensitive to clotrimazole. We also identified a  $\text{BK}_{\text{Ca}}$  channel with a  $210.4 \pm 5.8$  pS ( $n = 12$ ) conductance,  $\text{Ca}^{2+}$  dependent ( $K_{0.5} = 63.4 \pm 2.4$   $\mu\text{M}$ ,  $n = 8$ ) and sensitive to iberiotoxin and charybdotoxin. The  $\text{SK}_{\text{Ca}}$ , the  $\text{BK}_{\text{Ca}}$  and one of the  $\text{IK}_{\text{Ca}}$  channels characterized on bilayers, were very similar to the  $\text{K}_{\text{Ca}}$  channels, recorded by patch-clamp, regarding their unitary conductance, calcium dependence and kinetics, suggesting that they correspond to the same  $\text{K}_{\text{Ca}}$  channels. The presence of the  $\text{SK}_{\text{Ca}}$  ( $\text{SK}_3$ ) and the  $\text{BK}_{\text{Ca}}$  channels in the ciliary fraction was confirmed by Western blotting. On the other hand, the voltage-dependent  $\text{Na}^{+}$  channel was not detected, indicating the high purity of the ciliary membranes. Our biophysical and pharmacological characterization of the ciliary  $\text{K}_{\text{Ca}}$  channels in bilayers would allow a better understanding of their contribution to the  $\text{K}_{\text{Ca}}$  current in the inhibitory response in olfactory neurons.

Delgado R et al. (2003). *J. Neurophysiol* **90**, 2022–2028.

Supported by Fondecyt Grant 1020964

Where applicable, the experiments described here conform with Physiological Society ethical requirements.

## PC90

### Mutation of the alanine residue, A237 abolishes sensitivity of the tandem pore $\text{K}^{+}$ channel TASK-1 to extracellular pH

I. Ashmole, K. Yuill and P. Stanfield

Dept. of Biological Sciences, The University of Warwick, Coventry, UK

The pH dependence of the TASK channel sub-family is at least partly regulated by protonation of the side chain of a histidine residue (H98) which lies just beyond the consensus sequence for  $\text{K}^{+}$  selectivity in P1 (Kim et al. 2000; Ashmole et al. 2001). Previously we have reported that mutation of other residues located both inside the pore region e.g. isoleucine 94 in TASK-3 (Johnson et al. 2004) and outside e.g. glutamate 182 in TASK-1 (Ashmole et al. 2004) results in TASK channels with reduced sensitivity to extracellular pH. However, these channels also have significantly increased permeability to  $\text{Rb}^{+}$  and  $\text{Na}^{+}$  suggesting some disruption to the selectivity filter. Here we report the effect on ionic selectivity and pH sensitivity of mutation of a conserved alanine (A) residue, A237 (de la Cruz et al. 2003), located distal

to the selectivity filter, at the cytoplasmic end of transmembrane domain M4.

Murine TASK-1 channels were expressed in oocytes taken from *Xenopus* frogs that had been anaesthetised by immersion in 0.3% w/v MS222 and killed by destruction of the brain and spinal cord. We used two-electrode voltage clamp to investigate ionic selectivity and pH sensitivity. Ionic selectivity was calculated by measuring the shift in reversal potential when  $K^+$  in the external medium was replaced by  $Rb^+$  or  $Na^+$ .

The mutation A237T had no effect on channel selectivity. In oocytes expressing wild type channels  $PRb/PK$  was  $0.77 \pm 0.02$  ( $n = 9$ ; mean  $\pm$  SEM) and  $PNa/PK$  was  $0.04 \pm 0.003$  ( $n = 16$ ). For A237T neither the  $PRb/PK$  of  $0.79 \pm 0.02$  ( $n = 5$ ) nor the  $PNa/PK$  of  $0.05 \pm 0.004$  ( $n = 5$ ) was significantly different to wild type (ANOVA) indicating that the selectivity filter of the mutant channel remains intact. Remarkably however the mutant channels showed no sensitivity to extracellular pH over the physiological range. Whereas wild type channels are largely shut at pH6,

mutant channels remain open. This effect is most striking at positive membrane potentials; at +100mV  $IK(pH6)/IK(pH8.5) = 0.99 \pm 0.03$  ( $n = 7$ ). Even at -100mV,  $IK(pH6)/IK(pH8.5) = 0.88 \pm 0.04$  ( $n = 7$ ).

Our results show that the response to acidification of TASK-1 cannot simply be due to channel blockage by protonation of the histidine (H98) side chain but rather must involve a gating process.

Ashmole, I. *et al.* (2001). *Pflügers Arch* 442:828-833

Ashmole, I. *et al.* (2004). *J. Physiol.* 558P PC30

De la Cruz, I. *et al.* (2003). *J. Neurosci.* 23:9133-9145

Johnson, N. *et al.* (2004). *J. Physiol.* 558P PC31

Kim, Y. *et al.* (2000). *J. Biol. Chem.* 275:9340-9347

We thank the BBSRC for support.

*Where applicable, the experiments described here conform with Physiological Society ethical requirements.*